

## Heterogeneous catalytic synthesis of poly(butylene succinate) by attapulgite-supported Sn catalyst

Shiquan Lai, Yan Gao, Li Yue

School of Chemical Engineering, University of Science and Technology Liaoning, Anshan, Liaoning 114051, People's Republic of China

Y.G. performed the experiments, analyzed the data and wrote the manuscript. S.L. conceived and designed the experiments. L.Y. played an important role on the analysis of the data.

Correspondence to: S. Lai (E-mail: laishiquan@ustl.edu.cn)

**ABSTRACT:** An attapulgite-supported Sn catalyst (Sn-palgorските) was successfully prepared by ion-exchange co-impregnation method. The catalytic effect of Sn-attapulgite on the melt polycondensation reaction of poly(butylene succinate) (PBS) was examined by comparing with that of anhydrous SnCl<sub>2</sub> and a blank experiment. The structures and properties of the PBS products synthesized with the three catalytic systems were characterized by means of Fourier transform-infrared spectra (FT-IR), viscosity measurements, wide angle X-ray diffraction (WARD), differential scanning calorimetry (DSC), and thermogravimetric analysis (TGA). Meanwhile, the acidolysis degradation behaviors of the PBS samples were also studied. It was found that the intrinsic viscosities and the number-average molecular weights of the PBS were remarkably increased under the catalysis of Sn-attapulgite, further leading to an increase in the decomposition temperature, the crystallization temperature, and the viscous flow activation energy, while a decrease in the melting temperature, the relative degree of crystallinity, and the rate of degradation. Additionally, no significant differences were observed in the crystal structures of all the samples, regardless of the reaction system with or without catalyst. The experiment results confirmed that Sn-attapulgite was an effective heterogeneous catalyst for the synthesis of PBS, and the recycled Sn-attapulgite still exhibited higher activity than anhydrous SnCl<sub>2</sub> under identical reaction conditions. © 2014 Wiley Periodicals, Inc. *J. Appl. Polym. Sci.* **2015**, *132*, 41729.

**KEYWORDS:** catalysts; polycondensation; recycling

Received 27 August 2014; accepted 11 November 2014

DOI: 10.1002/app.41729

### INTRODUCTION

Plastics made of synthetic polymers are extensively used in our life. The increased consumption of plastics has resulted in producing a great deal of plastic wastes.<sup>1</sup> However, due to the undegradability of conventional polymers, these accumulating plastic wastes have severely polluted our survival environment. In order to solve the environmental pollution problems caused by waste plastics, as we have expected, more and more researchers nowadays have paid their efforts to develop biodegradable polymers that can be degraded to CO<sub>2</sub>, CH<sub>4</sub>, H<sub>2</sub>O, or other natural substances by microorganisms present in soil and water,<sup>2,3</sup> and eventually hope to replace traditional and nondegradable polymers such as polyethylene (PE), polypropylene (PP), and polystyrene (PS) with the degradable polymers.<sup>4</sup>

As a class of environment-friendly biodegradable polymers, aliphatic polyesters have attracted increasing attention because of their biodegradability, acceptable mechanical strength, favorable thermal stability, and processability.<sup>5,6</sup> They can be fabricated into various products such as fibers, films, sheets, nonwovens,

bottles, etc.<sup>7</sup> Studies on aliphatic polyesters is dated back to 1930s.<sup>8</sup> According to their chemical structure, aliphatic polyesters may be subdivided into two classes: one is prepared from hydroxyl acids by ring-opening polymerization and another is based on alkanedios and aliphatic dicarboxylic acids by polycondensation processes.<sup>9</sup> In general, the synthesis is commercially produced by the melt polycondensation of aliphatic dicarboxylic acid and diol compounds at 200 to 250 °C under highly reduced pressure.<sup>10</sup>

Poly(butylene succinate) (PBS), one of the most promising biodegradable aliphatic polyesters, is synthesized by the melt polycondensation of succinic acid and 1, 4-butandiol.<sup>11</sup> With excellent melt processability and thermal and chemical resistance, PBS can be fabricated into various products such as fibers, film, bottles, and injection-molded products. PBS which belongs to petroleum based polymers are also easily adaptable for mass production.<sup>2</sup>

However, the low melting points of the most produced polyesters in combinations with the difficulty to obtain high molecular weight materials has prevented their usage for long time. So, high

molecular weight polyesters are an essential request for producing materials with appropriate processability and acceptant mechanical properties.<sup>12</sup> Many studies have been carried on the using of chain extenders to prepare high molecular weight polyesters such as diisocyanates and diphenyl carbonates, with hydroxy terminated pre-polymers from diacids and diols, but this method is limited because of toxic chain extenders.<sup>13</sup> Nowadays, commercial synthetic processes are expected to be simple and economical. So it is very important to develop an easy synthetic process to manufacture high molecular polymers. Catalyst plays a critical role in enhancing the rate of the polycondensation reaction to effect the molecular weight of product,<sup>14</sup> so studying the catalyst used in the synthetic processes of polyesters is significant. Lahcini *et al.* studied the catalytic performance of chlorates on synthesis of PBS. The study found that the intrinsic viscosity of PBS catalyzed by  $ZnCl_2$  was 0.36 to 0.37 dL/g and that of PBS catalyzed by  $MgCl_2$  and  $BiCl_3$  is respectively 0.24 to 0.25 dL/g and 0.33 to 0.61 dL/g.<sup>9</sup> The PBS with intrinsic viscosity up to 0.69 dL/g was prepared by Ishii *et al.* in the presence of  $SnCl_2$  as catalyst.<sup>13</sup> However, the above catalysts belong to homogeneous catalyst and are difficult to be separated from product and recycle, causing environmental pollution and waste of resources. So it is imminent to find a heterogeneous catalyst that accord with green chemistry by allowing easy separation of the products and permitting the recycling and reuse of the catalyst with operational and economical advantages.<sup>15</sup> And it was found that there is no report on the synthesis of the PBS with heterogeneous catalyst so far.

Palygorskite (or attapulgite), a family of 2:1 hydrated magnesium aluminum silicate clay mineral, is characterized by a porous crystalline structure containing continuous two-dimensional tetrahedral sheets alloyed together by longitudinal sideline chains.<sup>16</sup> A theoretical unit cell consists of  $(Mg, Al, \text{ and } Fe)_5(Si_8O_{20})(OH)_2(H_2O)_4 \cdot 4H_2O$ , with Mg Preferentially located in octahedral sites.<sup>17</sup> These mineral clays possess Mg, Al, and Fe cations that can be easily exchanged.<sup>15</sup> Due to its fibrous morphology and higher specific surface area, attapulgite received a considerable attention as catalyst carriers and adsorbents.<sup>16,18</sup> Zhao *et al.* also used calcination combined with acid-activation to modify attapulgite and produced copper modified attapulgite catalysts ( $Cu^{2+}$ -PG/TiO<sub>2</sub>).<sup>19</sup> Lei *et al.* modified attapulgite with  $SnCl_2$  to prepare Sn-attapulgite catalyst and investigated its catalytic performance on ring ketones Baeyer-Villiger oxidation reaction.<sup>15</sup> Attapulgite-supported aluminum oxide hydroxide catalyst was prepared to catalyze the synthesis of poly(ethylene terephthalate) by Lin *et al.* and the new catalyst exhibited higher activity under identical reaction conditions.<sup>20</sup>

In this article, attapulgite-supported Sn complexes was prepared as heterogeneous catalyst. PBS was prepared respectively without catalyst, homogeneous catalyst ( $SnCl_2$ ) as catalyst, and heterogeneous catalyst (Sn-attapulgite) as catalyst. The structures of the synthesized PBS were characterized and its performance was investigated. The catalytic mechanism of catalyst and the effect on the reaction rate was also studied.

## EXPERIMENTAL

### Materials

Attapulgite clay powder was kindly supplied by Anhui Mingmei Minerals Co. Ltd. (Anhui Mingguang, China). Anhydrous  $SnCl_2$

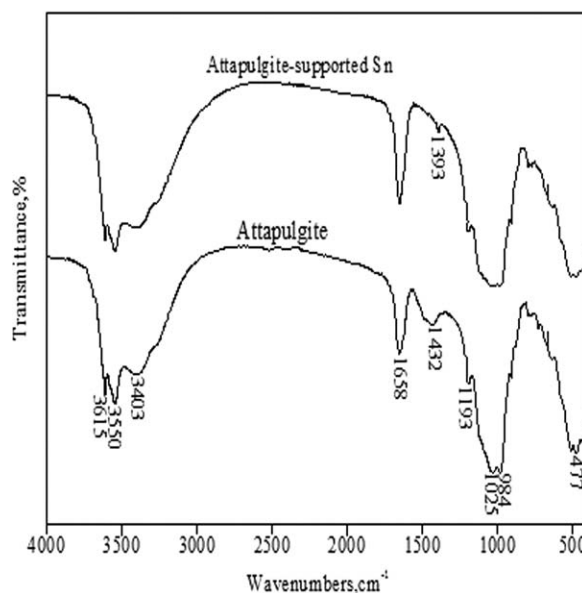


**Figure 1.** FT-IR spectra of attapulgite and attapulgite-supported Sn catalyst.

(purity 99%) and  $SnCl_2 \cdot 2H_2O$  (purity 99%) were purchased from Aladdin Reagent Company (Beijing, China). While 1,4-butanediol (BD, purity  $\geq 99\%$ ) and succinic acid (SA, purity  $\geq 99.5\%$ ) were purchased from Sinopharm Chemical Reagent Co., Ltd. (Shanghai, China). All the other reagents used in this experiment were of analytical grade and used as received without further purification.

### Preparation of Attapulgite Supported Sn Catalyst

The attapulgite-supported Sn catalyst was prepared according to the procedure similar to that reported by Lei *et al.*<sup>15</sup> The detailed preparation process can be described as follows: 1 g of the attapulgite powder was dispersed in 20 mL of 1 mol L<sup>-1</sup> HCl solution and vigorously stirred with the aid of ultrasonic wave for 2 h. Afterwards, 2 g of  $SnCl_2 \cdot 2H_2O$  was added to the mixture and the resultant slurry was again stirred for 24 h at room temperature. The products were collected by filtration, washed with a large number of ethanol and distilled water until no chloride anions could be detected ( $Ag^+$  test), and ground into  $<75 \overline{M}_n$  after drying at 105 °C in vacuum. The content of Sn in the catalyst is 2.32 wt % according to ICP analysis.

Figure 1 shows the FT-IR spectra of parent attapulgite and Sn-attapulgite. In the spectrum of attapulgite, the bands at 3615 and 3550  $cm^{-1}$  are attributed to the OH stretching vibration in (Al, Fe, and Mg)-OH. The band at 3403  $cm^{-1}$  is assigned to the OH stretching vibration of adsorbed and zeolitic water.<sup>21</sup> The Lewis and Bronsted acid sites are situated at 1658 and 1432  $cm^{-1}$ , respectively.<sup>15</sup> The bands in the low frequency region are due to Si-O and Si-O-Si vibrations. There are obvious changes in the spectrum of Sn-attapulgite compared to that of attapulgite. The peak at 1432  $cm^{-1}$  is shifted to 1393  $cm^{-1}$  and almost disappears. It may be attributed to the attapulgite inlaid with tin.

### Synthesis of PBS

PBS was synthesized via a two-stage melt polycondensation procedure, including esterification and transesterification. Typically,

0.1 mol of SA, 0.11 mol of BD, and a designated amount of attapulgite-supported Sn catalyst (about 2 wt % of SA) were charged into a 100 mL of four-necked glass flask equipped with a stirrer, water separator and N<sub>2</sub> inlet and outlet pipes. The mixture was quickly heated to 160°C under N<sub>2</sub> atmosphere and stirred for 1 h to finish the esterification. Subsequently, the reaction pressure was reduced to less than 4 kPa in 1 h, and the reaction temperature was raised up to 230°C to initiate the polycondensation. The polycondensation reaction time was ranged from 0 h to 5 h. After the end of the synthesis, the crude product containing catalyst particles was cooled to room temperature and dissolved in 75 mL of chloroform. The solid-liquid mixed solution was filtrated by a Buchner funnel. The filtrate was poured into 250 mL of cold methanol. The white precipitated product obtained was dried to constant weight in vacuum oven and named Sn-attapulgite-PBS. The solid catalyst particles collected was reused after drying.

For comparison, the PBS was respectively prepared without catalyst and with anhydrous SnCl<sub>2</sub> by the same procedure. The corresponding products were named no catalyst-PBS and SnCl<sub>2</sub>-PBS.

### Characterization

**Intrinsic Viscosity.** Intrinsic viscosity  $[\eta]$  measurements were carried out by using an Ubbelohde viscometer thermostated at 25°C in CHCl<sub>3</sub>. Intrinsic viscosity was calculated by the Solomon-Ciuta equation:<sup>22</sup>

$$[\eta] = \{2[t/t_0 - \ln(t/t_0) - 1]\}^{1/2}/C \quad (1)$$

where  $C$  is the concentration of the CHCl<sub>3</sub> solution,  $t$  is the flow time of the CHCl<sub>3</sub> solution, and  $t_0$  is the flow time of CHCl<sub>3</sub> solvent.

The number-average molecular weight ( $\overline{M}_n$ ) of the samples was calculated from  $[\eta]$  values, using the Berkowitz equation:<sup>22</sup>

$$\overline{M}_n = 3.29 \times 10^4 [\eta]^{1.54} \quad (2)$$

**Fourier Transform-Infrared Spectroscopy.** FT-IR spectra were recorded in the region 4000 to 400 cm<sup>-1</sup> in a Nicolet-550 infrared Fourier transform spectrometer, using the KBr pellet technique (about 1 mg of sample and 200 mg of KBr were used in the preparation of the pellets).

**Wide Angle X-ray Diffraction.** Wide angle X-ray diffraction patterns were obtained by using a PANalytical X'Pert diffraction with Cu K $\alpha$  radiation at room temperature with a scan rate of 2°·min<sup>-1</sup> from 5° to 90°. The degree of crystallinity ( $X_c$ ) was calculated using MDI Jade 6.0 software with sub-peak fitting function according to the procedure reported by Zhu *et al.*<sup>23</sup> The average crystal size ( $D_{\text{hkl}}$ ) was estimated by the following Scherer formula:

$$D_{\text{hkl}} = K\lambda/\beta\cos\theta \quad (3)$$

where  $K$  is Scherer constant (0.89),  $\lambda$  is the X-ray wavelength corresponding to the Cu-K $\alpha$  radiation (1.54056 Å),  $\beta$  is the half-height width of the diffraction peak, and  $\theta$  is the diffraction angle.

**Apparent Viscosity.** In order to study the rheological characteristics of the samples, the apparent viscosity was measured by a

rotational viscometry technique using a Model DV2TRV Digital viscometer manufactured by Brookfield Engineering Laboratories, INC. A SC4-29 spindle was selected for testing and its rotational speed was 20 rad s<sup>-1</sup>.

**Thermal Stability.** The thermal stability of the samples was determined by a TG-DTA 6300 thermogravimetric analyzer (TGA). All measurements were carried out at a heating rate of 10°C min<sup>-1</sup> from ambient temperature to 600°C under a nitrogen flow rate of 40 mL min<sup>-1</sup>.

### Thermal Properties

The melting temperature ( $T_m$ ), the fusion heat ( $\Delta H_m$ ) and the crystallization temperature ( $T_c$ ) of the samples were measured by a TA Company Q20 differential scanning calorimeter (DSC). About 5 mg of samples were placed in aluminum pans with a pierced lid. The tests were carried out under nitrogen atmosphere at a heating rate of 10°C min<sup>-1</sup> up to 160°C, and kept at this temperature for 5 min to eliminate the effect of the previous thermal history before crystallization; the melt was then dropped to room temperature at a cooling rate of 10°C min<sup>-1</sup>. The crystallinity  $X_c$  (%) of the sample was calculated according to the following equation:<sup>24</sup>

$$X_c = \frac{\Delta H_m}{\Delta H_m^0} \times 100\% \quad (4)$$

where  $\Delta H_m$  is the measured heat of fusion and  $\Delta H_m^0$  is the heat of fusion of a perfect crystal of PBS, which is assumed to be 210 J g<sup>-1</sup>.<sup>24,25</sup>

### Acidolysis Degradation

The acidolysis degradation was performed in HCl solution (5 wt %) at room temperature. The sample blocks were dried at 60°C for 48 h in vacuum before testing, and then put into the HCl solution. After degradation for a predetermined time, the samples were taken out of the medium, washed with distilled water and finally vacuum-dried to a constant weight at 60°C. The weight loss of the sample ( $w_{\text{loss}}$ ) was calculated from the following equation to express the acidolysis degradation rate of the samples:

$$w_{\text{loss}} = \frac{w_0 - w_1}{w_0} \times 100\% \quad (5)$$

where  $w_0$  and  $w_1$  are the weight of the samples before and after degradation in HCl solution, respectively.

## RESULTS AND DISCUSSION

### FT-IR Analysis

Figure 2 gives the FT-IR spectra of no catalyst-PBS, SnCl<sub>2</sub>-PBS, and Sn-attapulgite-PBS synthesized at 230°C for 5 h. The three infrared curves look very similar. The wide band at 3439 cm<sup>-1</sup> is attributed to the O-H stretching vibration. The bands at 2946 and 2854 cm<sup>-1</sup> are assigned to the C-H stretching vibrations of methylene group. The strong band at 1718 cm<sup>-1</sup> is due to the C=O stretching vibration. The band at 1156 cm<sup>-1</sup> is corresponded to the C-O stretching vibration. So it is obvious that a large number of ester bonds exist in the synthetic products. As it was expected, these results proved that the esterification of SA and BD did occur to produce PBS with or without a catalyst. Moreover, it can be noted that the

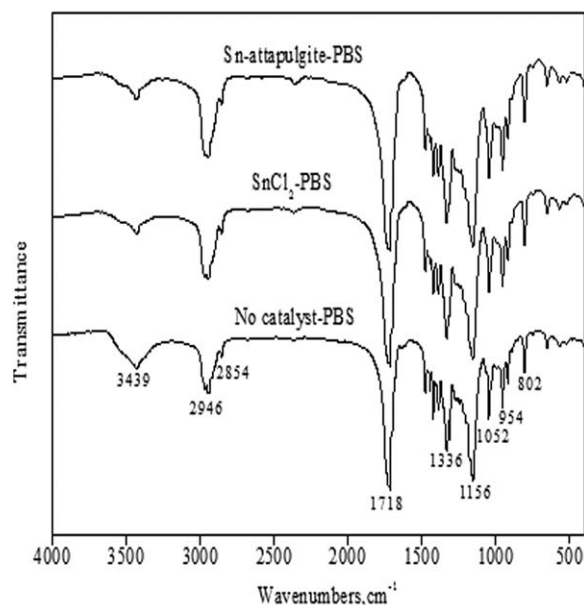


**Figure 2.** FT-IR spectra of no catalyst-PBS, SnCl<sub>2</sub>-PBS, and Sn-attapulgit-PBS.

characteristic peak intensity of ester bonds in the SnCl<sub>2</sub>-PBS and Sn-attapulgit-PBS are slightly stronger than that in the neat-PBS.

### Reaction Characteristics

In order to study the polycondensation reaction characteristics of PBS in the presence or absence of catalyst, the intrinsic viscosity values of all samples obtained at 230°C were measured and are presented in Figure 3. As it was expected, the intrinsic viscosity increases gradually with polycondensation time in the three reaction systems. The increase of intrinsic viscosity for no catalyst-PBS is from 0.19 dL/g to 0.26 dL/g, while for SnCl<sub>2</sub>-PBS from 0.21 dL/g to 0.62 dL/g and for Sn-attapulgit-PBS from 0.25 dL/g to 0.79 dL/g after 5 h of polycondensation. The additive of SnCl<sub>2</sub> or Sn-attapulgit used as catalyst can result in an obvious increase in intrinsic viscosity. At the same polycondensation time, the Sn-attapulgit-PBS exhibits the highest intrinsic viscosity in the three kinds of PBS samples. In addition, it is found in this experiment that the intrinsic viscosity of the PBS product synthesized at 230°C for 5 h using attapulgit powder as catalyst is only 0.33 dL/g.

Based on the  $[\eta]$  values of PBS samples, its number-average molecular weight ( $\overline{M}_n$ ) and number-average degree of polymerization ( $\overline{X}_n$ ) and the extent of reaction ( $P$ ) can be calculated respectively. The calculated results were summarized in Table I. It is clear from Table I that in the case of all three PBS samples, the value such as  $\overline{M}_n$ ,  $\overline{X}_n$ , or  $P$  increases as the polycondensation time at 230°C increases, but the increment of these values in the catalytic systems with time are much higher than that in the system without catalyst. At the same time, it is interesting to note that the PBS prepared with Sn-attapulgit catalyst has the highest value of  $\overline{M}_n$ ,  $\overline{X}_n$ , or  $P$  in the three PBS samples at all polycondensation times, suggesting that Sn-attapulgit is an excellent catalyst for the synthesis of PBS.

Flory theory indicates that the reactivity of the functional group does not depend on the size of molecule in polyesterification reaction. External-catalyzed polyesterification reaction can be expressed as a second-order rate law in the case of stoichiometric ratio of the functional groups and the rate law of such polyesterification is expressed as the following equation:<sup>26,27</sup>

$$\frac{1}{C_t} - \frac{1}{C_0} = kt \quad (6)$$

where  $C_0$  and  $C_t$  are the concentration of carboxyl groups at  $t = 0$  and  $t = t$ , respectively.  $t$  is reaction time and  $k$  is the rate constant. If the volume change of reaction system can be ignored during polycondensation reaction, then  $C_0$  and  $C_t$  are replaced by  $N_0$  and  $N_t$ , the eq. (6) can be expressed as follows:

$$\frac{1}{N_t} - \frac{1}{N_0} = kt \quad (7)$$

where  $N_0$  and  $N_t$  the mole number of carboxyl groups at  $t = 0$  and  $t = t$  during polycondensation reaction, respectively.

For unit mass of linear polyester, the molar number of functional groups  $N$  is defined as:

$$N = 1/\overline{M}_n \quad (8)$$

Hence, substitution of eq. (8) into eq. (7) obtains:

$$\overline{M}_n^{(t)} - \overline{M}_n^{(0)} = kt \quad (9)$$

where  $\overline{M}_n^{(0)}$  and  $\overline{M}_n^{(t)}$  are the number-average molecular weight of sample obtained at  $t = 0$  and  $t = t$  during polycondensation reaction, respectively.

In this research, based on the  $\overline{M}_n$  data in Table I, plots of the left side in eq. (9) against  $t$  are shown in Figure 4. Nearly straight lines are obtained for all the cases. The slopes of the straight lines shown in Figure 4 are determined by the least-squares method. The rate constants are obtained from the slopes as tabulated in Table I. It is found that the rate constant

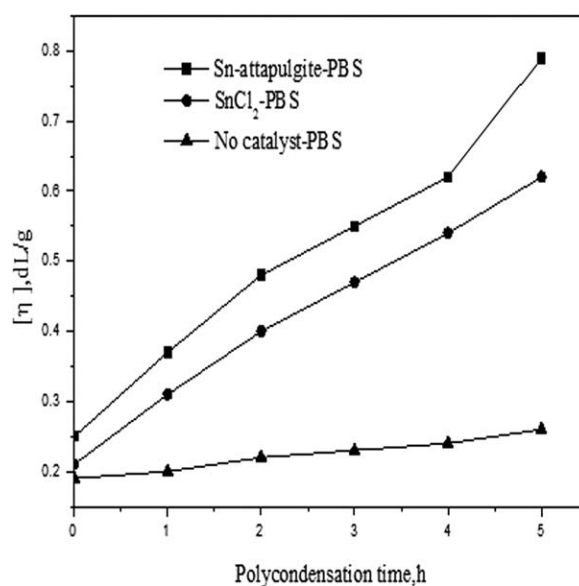


**Figure 3.** Variation of intrinsic viscosity with time during polycondensation of no catalyst-PBS, SnCl<sub>2</sub>-PBS, and Sn-attapulgit-PBS.

**Table I.** Number-Average Molecular Weight ( $\bar{M}_n$ ) and Degree of Polymerization ( $k$ ) of No Catalyst-PBS, SnCl<sub>2</sub>-PBS, and Sn-attapulgit-PBS Obtained at 230 °C for Different Times

Sample	Time (h)	$\bar{M}_n$	$\bar{X}_n$	$P$	$k$ (g mol <sup>-1</sup> min <sup>-1</sup> )
No catalyst-PBS	0	2250	13.08	0.924	6.27
	1	2760	16.05	0.938	
	2	3195	18.58	0.946	
	3	3420	19.88	0.950	
	4	3580	20.81	0.952	
SnCl <sub>2</sub> -PBS	0	2974	17.29	0.942	42.22
	1	5420	31.51	0.968	
	2	9376	54.52	0.981	
	3	10,290	59.83	0.983	
	4	12,864	74.80	0.987	
Sn-attapulgit-PBS	0	3890	22.62	0.956	56.87
	1	7120	41.40	0.976	
	2	10,624	61.77	0.984	
	3	13,100	76.16	0.987	
	4	15,851	92.16	0.989	
	5	22,992	133.67	0.993	

is 6.27 g mol<sup>-1</sup> min<sup>-1</sup>, 42.22 g mol<sup>-1</sup> min<sup>-1</sup>, and 56.87 g mol<sup>-1</sup> min<sup>-1</sup> for no catalyst-PBS, SnCl<sub>2</sub>-PBS, and Sn-attapulgit-PBS, respectively. The addition of SnCl<sub>2</sub> or Sn-attapulgit catalyst can make the polycondensation reaction of PBS speed 7 to 10 times.

### Crystalline Structures

The crystal structures of no catalyst-PBS, SnCl<sub>2</sub>-PBS, and Sn-attapulgit-PBS were characterized by wide-angle X-ray diffrac-

tion (WAXD). Figure 5 shows the WAXD patterns of the samples. The no catalyst-PBS sample exhibited three main characteristic diffraction peaks located at  $2\theta$  of 19.5, 22.5, and 28.9°, corresponding to (020), (110), and (111) planes, respectively. And the SnCl<sub>2</sub>-PBS and Sn-attapulgit-PBS showed the same characteristic diffraction peaks with no catalyst-PBS, indicating that the using of different catalyst did not change the crystal structure of PBS. The degree of crystallinity ( $X_c$ ) of the samples can be calculated through deconvolution of crystalline and amorphous peaks in the WAXD pattern using the peak

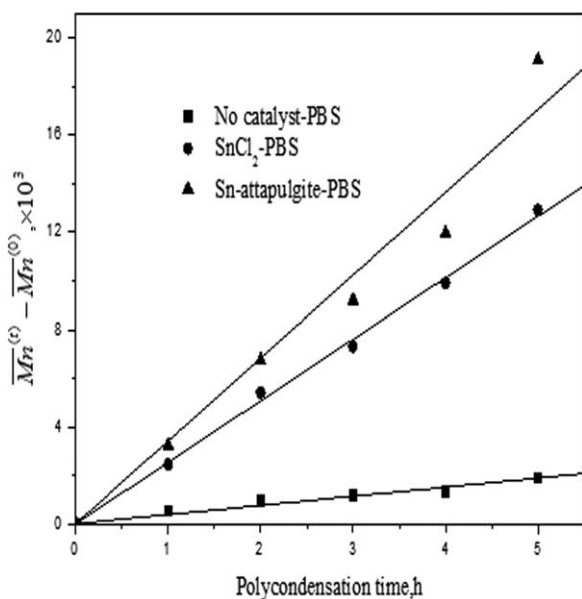


**Figure 4.** The relationship between the changing amount of molecular weight and polycondensation time.

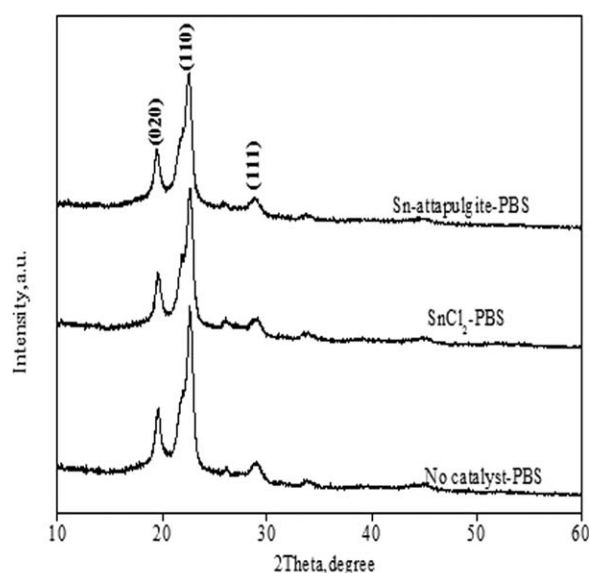


**Figure 5.** WAXD patterns of No Catalyst-PBS, SnCl<sub>2</sub>-PBS, and Sn-attapulgit-PBS.

**Table II.** The Half-Width (FWHM) of Diffraction Peak and Average Thickness in Vertical Direction of the Crystal Plane

Samples	Crystal plane index	$\beta$	$D_{hkl}/nm$	$X_c$ (%)
No catalyst-PBS	(020)	0.542	14.7162	52.56
	(110)	0.789	10.1604	
	(111)	0.936	8.6755	
SnCl <sub>2</sub> -PBS	(020)	0.545	14.6352	44.78
	(110)	0.813	9.8605	
	(111)	0.948	8.5656	
Sn-attapulgit-PBS	(020)	0.562	14.1925	41.53
	(110)	0.836	9.5892	
	(111)	0.982	8.2691	

separation software in the range of  $2\theta = 10$  to  $35^\circ$ .<sup>23</sup> The  $X_c$  values for no catalyst-PBS, SnCl<sub>2</sub>-PBS and Sn-attapulgit-PBS were 52.56%, 44.78%, and 41.53%, respectively, as shown in Table II. Considering the molecular weight of samples, the reason may be that the degree of entanglement between the polymer chains increases with increasing molecular weight and limit the rotation of the inner chain, affecting the movement of segments, thus affect the ordered pile of molecular chain and adversely affect the crystallization behavior of polymer.

Grain size directly affects the mechanical properties of polymer. The larger the grain size, the smaller the impact strength of material, the more easily broken.<sup>28</sup> Typically, X-ray diffraction method can also be used to calculate the grain size of the sample. It refers to the average thickness of the small crystal plane with the internal ordered arrangement in a direction normal. Since the actual thickness of the small crystal that generated diffraction is limited, the actual diffraction line broadened. They satisfy the Scherrer formula.

$$D_{hkl} = K\lambda/\beta\cos\theta \quad (10)$$

The half-width ( $\beta$ ) of diffraction peak and average thickness in vertical direction of the crystal plane are shown in Table II.

Table II shows the larger grain size of samples is no catalyst-PBS > SnCl<sub>2</sub>-PBS > Sn-attapulgit-PBS in each crystal plane. The reason may be that the melt viscosity increase with increasing molecular weight so the exercise capacity of polymer chains decrease to limit the chain segments to spread toward the nuclei and arrange resulting crystallization rate decreased. So the grain size becomes smaller with increasing molecular weight.

### Rheological Properties

In the molding process of polymer, it is important to have sufficient melt strength. The melt strength generally depends on the viscosity.<sup>29</sup> The apparent viscosities were measured in the temperature range of 140 to 170°C to evaluate the rheological properties of no catalyst-PBS, SnCl<sub>2</sub>-PBS, and Sn-attapulgit-PBS synthesized at 230°C for 5 h. The dependence of the apparent viscosity on temperature for the three PBS samples is illustrated in Figure 6. For all samples it is observed that the apparent viscosity decreases sharply with increasing temperature. At each

temperature, the apparent viscosity of Sn-attapulgit-PBS is much higher than that of no catalyst-PBS and SnCl<sub>2</sub>-PBS.

Based on the apparent viscosity ( $\eta$ ) values derived from Figure 6, the viscous flow activation energy  $E_\eta$  of the sample could be calculated according to the so-called Arrhenius-Eyring equation:

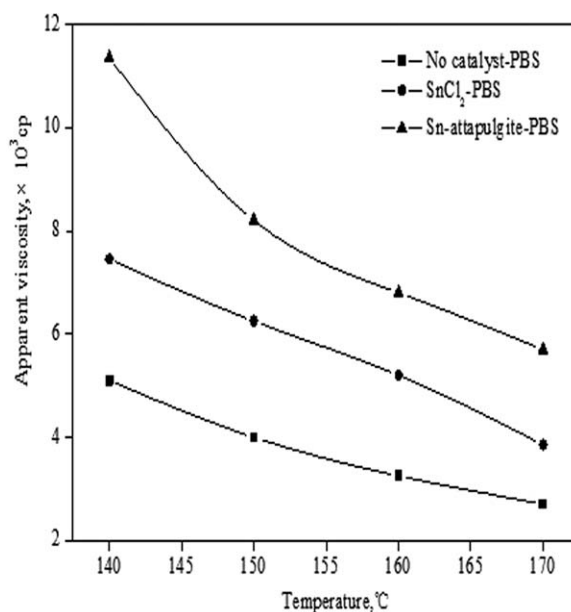
$$\ln\eta = \ln A + \frac{E_\eta}{RT} \quad (11)$$

where  $A$  is the pre-exponential constant,  $T$  is the temperature in Kelvin, and  $R$  is the universal gas constant.

The plots of  $\ln\eta$  against the reciprocal of the temperature ( $1/T$ ) for no catalyst-PBS, SnCl<sub>2</sub>-PBS, and Sn-attapulgit-PBS are shown in Figure 7. Nearly straight lines are obtained for all the samples. The best straight line is calculated with a correlation coefficient of 0.999 by the least-squares method. Since the slope gives  $E_\eta/R$ , we could obtain the viscous flow activation energy of the sample. The  $E_\eta$  values for no catalyst-PBS, SnCl<sub>2</sub>-PBS, and Sn-attapulgit-PBS are 33.42 kJ/mol, 33.67 kJ/mol, and 35.49 kJ/mol, respectively. So it is possible that the high molecular weight will result in high viscous flow activation energy.

### Thermal Stability of PBS

Thermal stability of PBS samples was studied by TGA. Figure 8 shows the TGA and DTG curves of no catalyst-PBS, SnCl<sub>2</sub>-PBS, and Sn-attapulgit-PBS. It is noted that the three PBS samples exhibit similar thermal decomposition behavior, and the temperature range of its obvious weight loss is about 300 to 400°C. The onset decomposition temperatures  $T_{0.05}$  (−5 wt %) for Sn-attapulgit-PBS is 316.6°C and that of SnCl<sub>2</sub>-PBS, No catalyst-PBS is respectively 310°C and 296°C, respectively. The maximum decomposing temperature  $T_{dm}$  of Sn-attapulgit-PBS is 381°C, and that of SnCl<sub>2</sub>-PBS, No catalyst-PBS is 370°C and 360°C, respectively. So it can be found that the PBS with Sn-attapulgit as catalyst possess more excellent thermal property.

**Figure 6.** Melt viscosities of Sn-attapulgit-PBS, SnCl<sub>2</sub>-PBS, and no catalyst-PBS at different temperature.

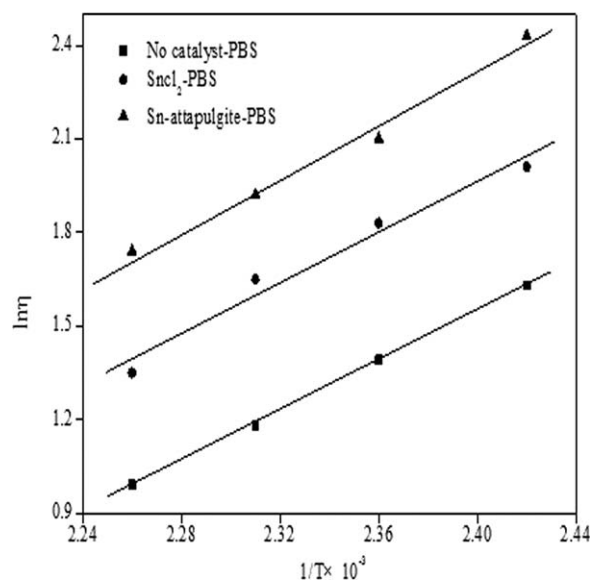


**Figure 7.** Plots of  $\ln \eta$  vs.  $\bar{X}_n$  for no catalyst-PBS, SnCl<sub>2</sub>-PBS and Sn-attapulgit-PBS.

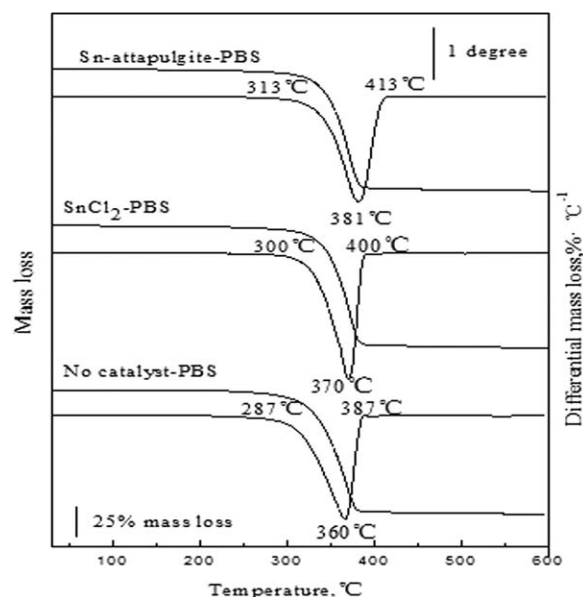


**Figure 8.** TGA curves of Sn-attapulgit-PBS and SnCl<sub>2</sub>-PBS.

### Thermal Properties of PBS

DSC analysis was used to investigate the thermal transitions and crystallization behaviors of the PBS samples. The first DSC heating scans, the cooling scans, and the second heating scans of PBS samples was showed in Figure 9. It is found that the three PBS samples show similar DSC thermograms, indicating there is no distinct difference in thermal property.

The characteristic data including crystallization temperature ( $T_{mc}$ ), crystallization enthalpy ( $H_c$ ), melting point temperature ( $T_m$ ), and fusion enthalpy ( $H_m$ ) are summarized in Table III. The  $X_c$  values are also obtained from the eq. (4). The result showed the crystalline degree of the PBS without catalyst was higher by 8.56% than that of the PBS with SnCl<sub>2</sub> as catalyst and that of PBS with Sn-attapulgit as catalyst was lowest (30.51%). And the order of higher crystallization temperatures was Sn-

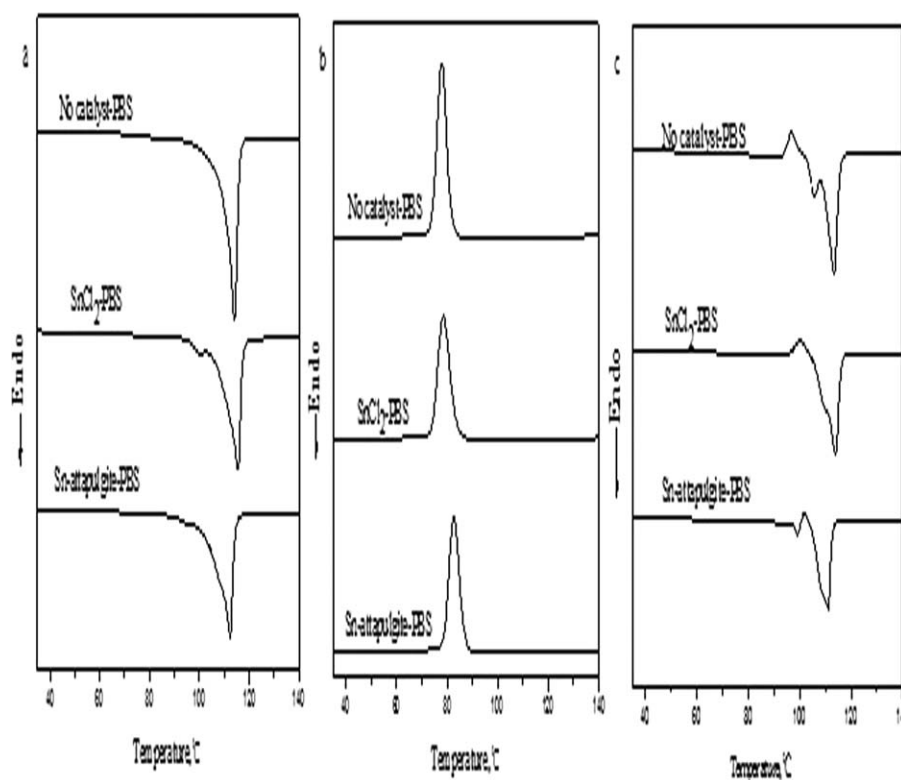


**Figure 9.** The first DSC heating scans (a), the cooling scans (b), and the second heating scans (c) of PBS samples.

**Table III.** Selected DSC-Results of No Catalyst-PBS, SnCl<sub>2</sub>-PBS, and Sn-Attapulgite-PBS

Sample	$T_m$ (°C)	$\Delta H_m$ (J/g)	$T_{mc}$ (°C)	$\Delta H_c$ (J/g)	$X_c$ (%)
No catalyst-PBS	110.72	87.25	81.46	87.25	41.54
SnCl <sub>2</sub> -PBS	109.91	69.26	83.36	73.09	32.98
Sn-attapulgite-PBS	106.80	64.08	86.75	70.69	30.51

attapulgite-PBS > SnCl<sub>2</sub>-PBS > no catalyst-PBS. It can be found that the melting temperatures of the PBS with Sn-attapulgite as catalyst was 106.80°C, and that of SnCl<sub>2</sub>-PBS (no catalyst-PBS) increased slightly by 3.11°C (3.92°C).

### Acidolysis Degradation

Acidolysis degradation was carried out in 5 wt % HCl solution at room temperature to evaluate the degradation properties of these PBS samples synthesized in different reaction systems. The weight remaining versus degradation time for the samples is graphically shown in Figure 10. Nearly same changes were observed for the three PBS samples. Namely, in the first stage of degradation (3 days), the weight loss of all PBS samples was very slow and less than 3 wt %. However, after 3 days the weight loss of these samples almost linearly increased with degradation time and finally became slow again after 9 days. This characteristic for the PBS degradation coincides well with that for autocatalytic type reactions. The weight loss of no catalyst-PBS in 12 days was 23.5 wt %, while that of SnCl<sub>2</sub>-PBS and Sn-attapulgite-PBS was 21.6 wt % and 16.3 wt %, respectively, suggesting that the degradation rate of PBS was relatively fast in the HCl solution compared to the data reported by Zeng *et al.*<sup>30</sup> in the phosphate buffered solution. In addition, it is apparent that Sn-attapulgite-PBS had the minimum weight loss

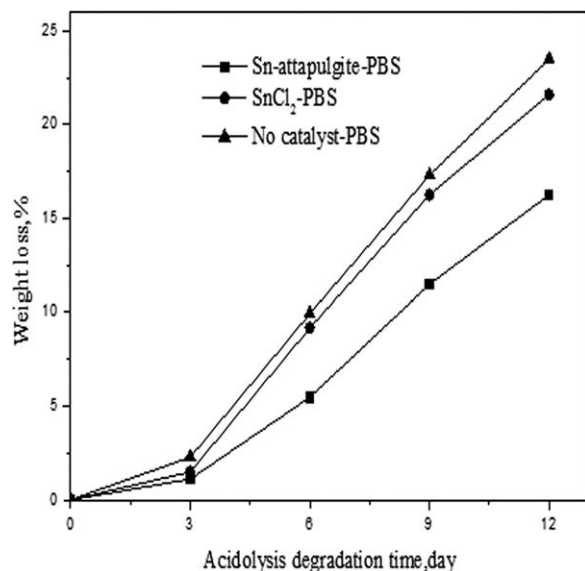


**Figure 10.** Acidolysis degradation of Sn-attapulgite-PBS, no catalyst-PBS, and SnCl<sub>2</sub>-PBS in hydrochloric acid solution (5 mas %) at room temperature.

in the same degradation time in the three PBS samples, which is attributed to its longest main chain with ester bonds.

### Catalyst Recycling

Sn-attapulgite complexes is light gray powder, while the used Sn-attapulgite was black. It can be found that the color of used Sn-attapulgite recover after it had been calcined in muffle furnace at 803 K for 8 h. So it can be inferred that carbon deposition was attached on the catalyst surface. To investigate the catalytic activity of recovered catalyst, PBS was prepared with the recovered catalyst as catalyst at the same condition. The result showed the inherent viscosity of PBS with the recovered catalyst was 0.6366 dL/g when the polycondensation time was 5 h. The result demonstrated the recovered catalyst still possess excellent catalytic activity compared to SnCl<sub>2</sub>.

### CONCLUSION

Sn-attapulgite was prepared by a simple procedure and shown to act as a highly active catalyst for the preparation of PBS. The prepared PBS possess high intrinsic viscosity, molecular weight, and excellent thermal performance. The rate of polycondensation reaction is significantly faster with Sn-attapulgite as catalyst. And Sn-attapulgite is easily separated from products and can be recycled. So Sn-attapulgite is an excellent catalyst not only on production process but also on economics and environmental protection.

### ACKNOWLEDGMENTS

The authors thank the financial support of the University of Science and Technology Liaoning.

### REFERENCES

1. Velmathi, S.; Nagahata, R.; Sugiyama, J. -I.; Takeuchi, K. *Macromol. Rapid Commun.* **2005**, *26*, 1163.
2. Shi, X. Q.; Aimi, K.; Ito, H.; Ando, S.; Kikutani, T. *Polymer* **2005**, *46*, 751.
3. Chen, C. -H.; Peng, J. -S.; Chen, M.; Lu, H. -Y.; Tsai, C. -J.; Yang, C. -S. *Colloid. Polym. Sci.* **2010**, *288*, 731.
4. Zeng, J. -B.; Huang, C. -L.; Jiao, L.; Lu, X.; Wang, Y. -Z.; Wang, X. -L. *Ind. Eng. Chem. Res.* **2012**, *51*, 12258.
5. Takasu, A.; Iio, Y.; Oishi, Y.; Narukawa, Y.; Hirabayashi, T. *Macromolecules* **2005**, *38*, 1048.
6. Lenz, R. W.; Marchessault, R. H. *Biomacromolecules* **2004**, *6*, 1.
7. Agarwal, S.; Wendorff, J. H.; Greiner, A. *Polymer* **2008**, *49*, 5603.
8. Carothers, W. H. *J. Am. Chem. Soc.* **1929**, *51*, 2548.
9. Lahcini, M.; Qayouh, H.; Yashiro, T.; Simon, P.; Kricheldorf, H. R. *J. Macromol. Sci. Part A: Pure Appl. Chem.* **2010**, *47*, 503.
10. Ito, H.; Yamamoto, N.; Hiroji, F.; Jojima, M. Japan Patent 71,641, March 18, **1997**.
11. Jeong, E. H.; Im, S. S.; Youk, J. H. *Polymer* **2005**, *46*, 9538.
12. Bikiaris, D. N.; Achilias, D. S. *Polymer* **2008**, *49*, 3677.



13. Ishii, M. M. O.; Shibasaki, Y.; Ueda, M. *Biomacromolecules* **2001**, *2*, 1267.
14. Dou, J.; Liu, Z. *Green Chem.* **2012**, *14*, 2305.
15. Lei, Z.; Zhang, Q.; Wang, R.; Maand, G.; Jia, C. *J. Organomet. Chem.* **2006**, *691*, 5767.
16. Lai, S.; Yue, L.; Zhao, X.; Gao, L. *Appl. Clay Sci.* **2010**, *50*, 432.
17. Brigatti, M. F.; Galán, E.; Theng, B. K. G. In *Handbook of Clay Science, Developments in Clay Science*; **2006**, *1*, pp. 19–86.
18. Miao, S.; Liu, Z.; Zhang, Z.; Han, B.; Miao, Z.; Ding, K.; An, G. *J. Phys. Chem. C* **2007**, *111*, 2185.
19. Zhao, D.; Zhouand, J.; Liu, N. *Appl. Clay Sci.* **2006**, *33*, 161.
20. Lin, Q.; Gu, Y.; Chen, D. *J. Appl. Polym. Sci.* **2013**, *129*, 2571.
21. Augsburger, M. S.; Strasser, E.; Perino, E.; Mercader, R. C.; Pedregosa, J. C. *Phys. Chem. Solids* **1998**, *59*, 175.
22. Solomon, O. F.; Ciuta, I. Z. *J. Appl. Polym. Sci.* **1962**, *6*, 683.
23. Zhu, Q. Y.; He, Y. S.; Zeng, J. B.; Huang, Q.; Wang, Y. Z. *Mater. Chem. Phys.* **2011**, *130*, 943.
24. Bikiaris, D. N.; Papageorgiou, G. Z.; Achilias, D. S. *Polym. Degrad. Stabil.* **2006**, *91*, 31.
25. Chen, C. -H.; Peng, J. -S.; Chen, M.; Lu, H. -Y.; Tsai, C. -J.; Yang, C. -S. *Colloid Polym. Sci.* **2010**, *288*, 731.
26. Lin, C. -C.; Hsieh, K. H. *J. Appl. Polym. Sci.* **1977**, *21*, 2711.
27. Uphade, B. S.; Patil, P. S.; Pandit, S. B.; Rajan, C. R.; Nadkarni, V. M. *J. Polym. Sci. Part A: Polym. Chem.* **1994**, *32*, 2003.
28. Jin, R.; Hua, Y. *Polymer Physics*; Chemical Industry Press: Beijing, **2006**; Chapter 2, p 45–46.
29. Lim, S. -K.; Jang, S. -G.; Lee, S. -I.; Lee, K. -H.; Chin, I. -J. *Macromol. Res.* **2008**, *16*, 218.
30. Zeng, J. -B.; Huang, C. -L.; Jiao, L.; Lu, X.; Wang, Y. -Z.; Wang, X. -L. *Ind. Eng. Chem. Res.* **2012**, *51*, 12258.